Flexural Behavior of Concrete Slabs Reinforced with Innovative Semi-Ductile Hybrid FRP Bars

Mohamed Abo Elyazed, Reham Eltahawy, Omar A. EL-Nawawy and Khaled S. Ragab

Abstract—This study introduces a new ductile hybrid reinforcement bar (Glass-Steel wires) fiber reinforced polymers (HFRP), steel hybrid bar with a core of steel wires, three types of the hybrid cross section with three different steel ratios of 6.25%,12.5% and 22% are considered. As a result of tensile tests, the elastic modulus of FRP Hybrid Bars is improved as 3.66% - 24.4% in comparison with the normal GFRP Bars. The bars are locally manufactured by double parts die template using local resources raw materials. A total of five slabs, measuring 800 mm wide x 150 mm thickness x 2400 mm long, simply supported are tested in the laboratory under static four-line loading conditions to determine their flexural limit states, including the behavior prior to cracking, cracking, ultimate capacities and modes of failure. The main parameters are the reinforcement material type (GFRP, steel and HFRP bars). The ultimate load decreased by 9.6 % as the reinforcement type (HFRP-C -14 Wires) compared with GFRP bars and produce some amount of ductility provided by the hybridization performance. A non- linear finite element analysis is conducted for the experimental program using ANSYS. This study investigates the structural behaviour of one-way hybrid reinforced concrete slab, for different reinforcement hybrid bars types.

Keywords: Hybrid FRP, locally produced, steel wires, Concrete Slabs, Flexural behaviour, Theoretical prediction, ANSYS.

1 INTRODUCTION

The corrosion of the conventional reinforcement steel bar is the main reason for the decline of reinforced concrete structures [1–4]. Many researches have been conducted, and numerous procedural methods have been proposed to solve the steel bar corrosion problem [5–12]. The American Concrete Institute's document (ACI 222R-85) [12] recommended three protection methods: 1) adding steel corrosion inhibitors, 2) coating steel bars with epoxy, and 3) providing cathodic protection. Prior studies found that the first method integrating steel rust inhibitors is effective for long-term corrosion resistance [12]. Although this method shows effective benefits in terms of cost, but the construction is more convenient compared to the other two technologies, its fundamental shortcomings limit its application. The another epoxy-coating method calls for coating the bars with a thin coating of epoxy using a static powder spray. This method provides excellent grip strength between the steel and concrete while producing good alkali and surface of a steel bar is imperfect due to some failings, such as its inner quality or breakage during transportation, local corrosion development is frequently faster than with uncoated steel, resulting in more serious corrosion degradation [5]- [11].

Mohamed Abo Elyazed, Teaching Assistant, Structural Engineering Department, October high institute for Engineering & Technology, Giza, Egypt.

Reham Eltahawy, Assistant Professor Concrete Structures Department, Faculty of Engineering Ain Shams University, Cairo, Egypt.

Omar A. El- Nawawy, Professor of R.C. Structures, Concrete Structures Department, Faculty of Engineering Ain Shams University, Cairo, Egypt.

Khaled S. Ragab, Professor of Reinforced Concrete Research Department, Housing and Building National Research Centre, Giza, Egypt.

In recent decades, engineers and researchers have considered the use of corrosion-resistant materials to integrate into concrete structures, such as fiber reinforced polymer (FRP) [13]- [18]. FRP materials have great properties, such as light weight, high strength, corrosion resistance, fatigue resistance, and low creep. FRP has also been used in the manufacturing of rebars, as an alternative to the conventional steel, However, although the FRP tapes have good applicability, shortcomings remain, which it retained by being the necessary support for large-scale concrete structures. These shortcomings include linear elasticity, low elastic modulus, and high cost [17,18]. To improve the performance of ductility and durability of concrete structures, researchers in recent years have proposed a new developed hybrid bar known as a hybrid FRP bars were presented to improve the elastic modulus and to improve the brittle failure, Nanni et al. (1994) [19], developed a hybrid rod consisting of FRP braided skin made up of aramid or vinylon fiber and a steel bar in core. It was found that the hybrid rod had a modulus of elasticity higher than that of the normal FRP bar and showed a bi-linear performance in ductile mode. A hybridization method was studied by Dong-Woo Seo et al. [21,22] and Minkwan Ju, et al (2017) [25], and noted that the hybridization of GFRP bar with a steel bar in core is developed to overcome the low elastic modulus of GFRP bar by hybridized process with steel. It showed an improvement in the modulus of elasticity.

In this study, the GFRP hybrid bar HFRP with exceptional properties such as non-corrosiveness and high modulus of elasticity is produced [21]- [29]. The hybrid bars HFRP can provide structural efficiency to the reinforced concrete having low crack width and deflection as compared to normal GFRP bars and show better serviceability in flexure. The hybrid bars HFRP also contribute to the durability of concretes due to non-corrosion of the GFRP surface. With concerning with the

structural design, numerous guidelines have been proposed for designing the reinforced concretes using GFRP bars (ACI 440.1R-15 2015 [33]; CSA S806-12 2012 [36] and ECP 208-2005 [38]). The material and mechanical characteristics of the GFRP hybrid bars can be studied and imitated in those structural designs.

Based on the HFRP properties and the conclusions from previous research [21], [22], [25] and [26], a unique type of HFRP rebar is proposed and developed by the first author, along with others, to achieve the required enhance of modulus and ductility. One of the objectives of this study is to conduct experiments on a series of slabs specimens reinforced with the proposed hybrid FRP rebars in order to investigate their mechanical properties and flexural behavior under static loading.

2 EXPERIMENTAL PROGRAM

2.1 Manufacturing Process of HFRP Rebars

Hybrid Innovative Semi-Ductile FRP Bars is manufactured at 10th of Ramadan Industrial City, 50 km away from Cairo, Egypt. This article introduces (HFRP) and these bars are developed to overcome the low elastic modulus of GFRP bar by hybridizing with steel. As shown in fig.1 three types of HFRP and one GFRP and steel bar are taken into consideration in this study:

(a) GFRP crust with four steel wires in the core of the cross section.
(b) GFRP crust with eight steel wires in the core of cross section;
(c) GFRP crust with fourteen steel wires in the core of cross section.

The HFRP bars are manufactured by the authors using glass fiber roving and unsaturated polyester resin. Double sets of plastic molds are manufactured at specific workshop to manufacture 2400 mm long HFRP bars with 12 mm diameter. The HFRP ribbed bar of 12 mm diameter and double sets of plastic molds manufactured be wood and glass fiber are shown in Fig.2.

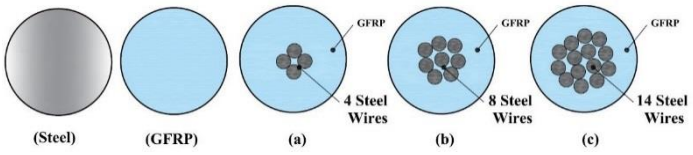

Fig. 1 Cross section types of Steel bar , GFRP bar and "FRP Hybrid Bars" [HFRP]

2.2 Tensile Tests of HFRP Rebars

Tensile tests are accomplished in accordance with ASTM D3916 [35]. The total length is 1000 mm and the gauge length was 400 mm. Due to the brittle nature of the GFRP bars, they typically fail in the gripped areas in tension test leading to inexact results. Hence, the design and development of the test specimens should contain suitable gripping mechanism to assure that the failure takes place far from the gripped zones. In this study the special protections mentioned in ACI 440.3R-12 [32] are applied.

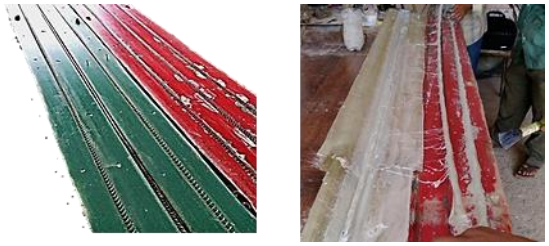

Fig. 2 Manufactured GFRP bars: Double sets of deformed plastic molds.

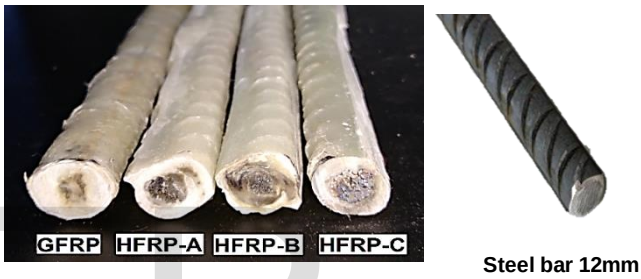

Fig. 3 Final product for development of GFRP ,HFRP Hybrid Bars and steel bar 12mm

The protections are to use steel tube end anchors on both ends of the tested bars to allow for uniform distribution of the load applied from the testing machine to the test specimen. The anchorage system, Fig. 4, composed of a steel tube of 30 mm and 22 mm external and internal diameter, respectively The steel tube was filled with a high-performance resin (Sikadur-31) grout to assure good bond between the bar and the steel tube. Fig.4 shows a schematic diagram of the details of the used anchorage system. And also shows a schematic diagram and the dimensions of typical test specimen.

The results of all bars from tension tests are presented below. These tests are conducted on the UH-1000 KN capacity universal machine as shown in Fig.5

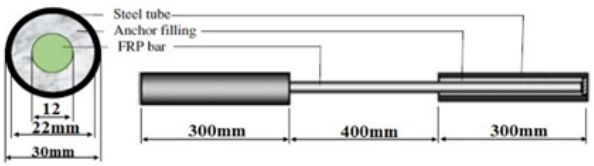

Fig. 4 Dimensions of typical test specimen

Fig. 5 Specimen and Tensile test setup

Fig. 6 HFRP with steel wires in core at failed in both glass and wires fiber

It is observed that all test specimens failed in the middle third of the specimen's length where the fibers broke and the damage spread throughout the specimen's length, as shown in Fig.6.

With reference to Fig.7 it is clear that the normal GFRP bars showed linear behavior until failure, the bars also showed a clear brittle failure. Fig.7, showed that the stress-strain behavior for bars which manufactured with hybrid glass / four steel wires (diameter 1.5 mm) with steel to glass fiber ratio 6.25 % (HFRP A), it showed linear behavior until a clear yielding occurred at load about 90 % the ultimate load. After yielding, the load-strain rate become clearly low and the load-strain curve deviated clearly towards the x-axis showing a clear semi-ductile behavior. Likewise, Fig.7 indicates that the bars manufactured with hybrid glass / eight steel wires (diameter 1.5 mm) with steel to glass fiber ratio 12.5 % (HFRP-B), showed a yielding zone at load about 84 % of the ultimate load, also the load strain rate turned to be clearly lower than after yielding.

The same behavior was observed for bars manufactured with hybrid glass / fourteen steel wires (diameter 1.5 mm) with steel to glass fiber ratio 22 % (HFRP-C), but with higher yield/ultimate loads ratio, the stress-strain behavior was linear until a clear yielding occurred at load about 95 % the ultimate load. After yielding, the load-strain rate was clearly low and the load-strain curve deviated clearly towards the x-axis showing a clear semi-ductile behavior.

2.3 Tensile Behavior Characteristics.

For the tensile test, the average of three specimens for every HFRP bar type, defined in Table 1, are tested. The tensile strength of the specimens can be calculated by dividing the

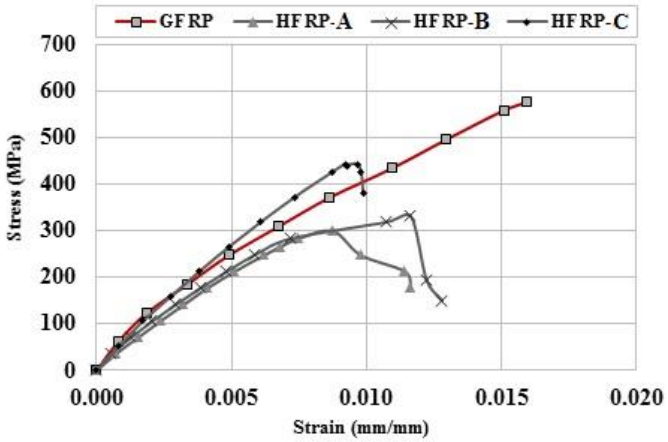

Fig. 7 Comparison between GFRP and HFRP (A, B and C)

measured maximum load over the cross-sectional area of FRP Hybrid Bar (A_{hybrid}). The elastic modulus of FRP Hybrid Bar (Ehybrid) can be given by the following expression as recommended in Canadian Standards association (CAN/CSA S806-12) [36], Test Method for Tensile Properties of FRP Reinforcement.

$$\mathbf{E_h} = \frac{(\mathbf{P_1} - \mathbf{P_2})}{(\boldsymbol{\varepsilon_1} - \boldsymbol{\varepsilon_2})\mathbf{A_h}} \qquad (1)$$

Where P_1 and ε_1 are the load and corresponding strain respectively, at approximately 50% of the ultimate tensile capacity, while P_2 and $\varepsilon 2$, are the load and corresponding strain respectively, at approximately 25% of the ultimate tensile capacity.

Table 1 summarizes the result of tensile tests for steel, GFRP and FRP Hybrid Bar (A, B and C) respectively. Most of the specimens failed in the area of the gauge length. Nine cases were tested associated with three different types and with various steel-to-GFRP volume ratios.

Also, table 1 summarizes the results of tensile tests for the hybrid bar specimens. The hybrid effect is stated in reference to the ultimate strain of the normal GFRP bar. Overall, the ultimate strains of the hybrid bars decreased by 30.8-57% compared to that of the normal GFRP bar for types which hybridization with steel bar (A, B and C).

2.4 Flexural behaviour of one-way slabs under static four- line loading

Five slabs are tested at the reinforced concrete laboratory at the Housing and Building National Research Center (HBNRC) [31], Cairo, Egypt. Table 2 shows complete details of the specimen cross-sections, type and ratio of the reinforcement and the special concrete strength for the five specimens. Five simply supported concrete slabs reinforced were tested in flexure, three slabs are reinforced with HFRP and one reinforced with GFRP, in addition to a slab reinforced with conventional steel rebars is also tested as a reference slab with GFRP slab.

Table 1 Characteristics Of Reinforcement Bars

TYPE OF BAR	Steel in core: Steel wires (1.5mm)	No. of Yarn (Glass)	Steel / GFRP ratio %	Ultimate Load: P_u (KN)	Elastic Modulus: Aver.(GPa	Elastic Modulus: Imp.(%)	Tensile Strength (MPa)	Ultimate Strain %	Ultimate Strain Imp.(%)
STEEL	--	--	100%	73.5	200	387.80	650.44	0.032	50.94
GF(REF.)	--	66	0%	65	41	--	575.22	0.0157	---
HFRP-A	4 wires	60	6.25%	33.8	42.5	3.66	299.12	0.011	-42.73
HFRP-B	8 wires	40	12.5%	38	46.53	13.49	330.97	0.012	-30.83
HFRP-C	14 wires	20	22%	50.4	51	24.39	442.48	0.01	-57

All tested slabs are 800 mm in width, 150 mm in depth and 2400 mm length. The simply supported slabs had a span of 1800 mm as shown in Fig. 8. A concrete cover of 20 mm thickness was kept constant for all specimens. The slab notation is defined according to the type of reinforcement. The first letter in the notation indicates the type of specimen, "S" for slabs. The second letter corresponds to the type of reinforcement, (S, G and H) for the type of reinforcement (steel, Glass FRP and Hybrid FRP, respectively). The third letter reflects the Hybrid FRP reinforcement type (A, B and C) as shown in Fig.3 and table 2. For example, the slab notation SHA indicates a slab reinforced with HFRP its type is GFRP crust with a four steel wires in the core.

All slabs are tested under four-line bending over a clear span of 1800 mm and a shear span of 700 mm, as shown in Fig.8. A hydraulic jack is used to apply a concentrated load on a steel distribution I-beam to produce two-point loading condition. Three LVDTs are used for each specimen to monitor the vertical displacements; one LVDT is located at mid-span, the two LVDTs are located at quarter-span. For each specimen, three electrical strain gauges of 10 mm length and 120-ohm resistance are attached to GFRP, HFRP and steel reinforcement at mid-span and quarter-points to monitor the bar strain during loading. Also, one external strain gages are attached directly to the concrete upper surface at mid-span to measure the maximum compressive strains in concrete, see Fig. 9.

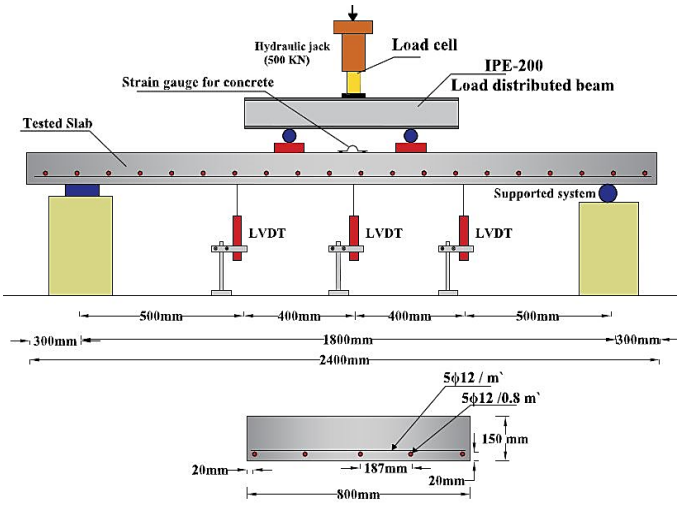

Fig. 8 Experimental details of HFRP slabs

Fig. 9 Flexural test setup of concrete slabs

3 TEST RESULTS AND DISCUSSION

3.1 Crack propagation and failure modes for the specimens

Cracks occur at the surface of the bottom of concrete slabs whenever the tensile stresses exceed the modulus of rupture of concrete Fig.10. The first crack appears at the middle of the slab and develops slowly across the width of the slab. Further development of cracks occurs, on increasing the application of load under static loading conditions. All the slabs experience flexural failure, the first visible cracking load of all slabs tested is presented in Table 3.

Fig. 10 Crack propagation

Two different failure modes were observed in the experimental tests as shown in Fig.11 and Fig.12, and summarized in Table 3 and explained below:

Table 2 Test Matrix

Slab Notation	Slabs dimensions		Effective Span, L (mm)	Reinforcement Rebar type		Concrete properties	
	Width, b (mm)	Depth, t (mm)		Type of bar	Bottom reinforcements	f_{cu} MPa	f_{ct} MPa
SS	800	150	1800	Steel	5Ø12/0.8m'	40	3.79
SG (REF)	800	150	1800	GFRP	5Ø12/0.8m'	39	3.75
SHA	800	150	1800	HFRP (A)	5Ø12/0.8m'	35	3.55
SHB	800	150	1800	HFRP (B)	5Ø12/0.8m'	36	3.6
SHC	800	150	1800	HFRP (B)	5Ø12/0.8m'	37	3.65

Mode 1:

Combined shear and flexure failure, this mode was experienced by slab SG and SHC, that was reinforced with an under-reinforcement ratio of ribbed-surface GFRP and HFRP-C bars at the mid-span region as shown in Fig.11, respectively. It should be noted that all tested slabs were tested under increasing static load up to failure.

It was observed that the first visible flexural cracks for slab SG and SHC appeared at loads of 27 kN and 28 KN, respectively.

However, a diagonal shear crack suddenly appeared which located outside the constant moment zone between the load location and quarter point location that widened and propagated to the vicinity of the applied load location and the support causing concrete crushing at the top surface of slabs, as shown in Fig.12 for slabs SG and SHC, respectively, leading to slab collapse. Failure of slabs SG and SHC occurred at an ultimate load of 88.5 kN and 80 kN, respectively, due to combined shear and bending.

Fig. 11 Flexure–shear failure at mid-span of slab SG

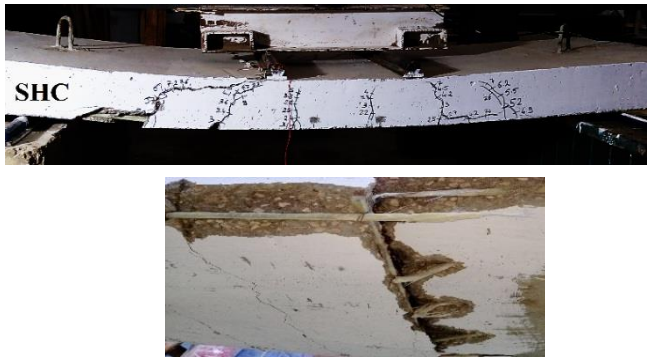

Fig. 12 Flexure–shear failure at mid-span of slab SHC

Mode 2:

Conventional ductile flexural failure–This mode occurred due to yielding of tensile steel and hybrid FRP reinforcement bar followed by concrete crushing at mid-span for all slabs except S-G and SHC as shown in Fig. 11 and Fig.12. The steel reinforced concrete slab exhibited a basic first cracking load higher than slabs reinforced with HFRP owing to the higher axial stiffness of steel bars than that of HFRP bars. The ratio of hybridization of each type of HFRP reinforcement bar at different slab tested has also affected the first cracking load.

Fig.14 and Fig.15 shown the crack pattern at failure of the slab SH (A and B) with ribbed-surface HFRP- (A and B) bars. It should be noted that all slabs are tested under increasing static load up to failure. It was observed that the first visible flexural cracks for slab SS, SHA and SHB appeared at loads of 32.5 KN, 28 KN and 31 KN, respectively. Failure of slabs SS, SHA and SHB occurred at an ultimate load of 122 KN,57 KN and 52 KN, respectively, due to flexure failure only.

Table 3 shows the experimental and theoretical crack load capacities of the slabs at the first crack appearance. The theoretical predictions are made in accordance with existing design guidelines.

Fig. 13 Ductile flexural failure mode of hybrid slab SS

Fig. 14 Ductile flexural failure mode of hybrid slab SHA

Fig. 15 Ductile flexural failure mode of hybrid slab SHB

Fig. 16 The effect of hybridization in overcome the sudden rupture for type (A,B and C)

$$M_{cr} = \left(\frac{f_{ctr}}{y_t} * I\right) * 10^{-6} \qquad (2)$$

where M_{cr} is the cracking moment, KN.m, F_{ctr} the modulus of rupture of concrete, N/mm², I the moment of inertia of slab section, mm⁴, and y_t is the distance from the centroid to extreme tension layer of the section, mm.

The moment of inertia of the slab section is considered as the moment of inertia of gross concrete section about centroid axis, neglecting the moments of inertia of all reinforcements.

Earlier research results have shown that the effect of FRP reinforcement ratio on the cracking moment is practically negligible due to the low modulus of elasticity of the FRP reinforcement [18]. The modulus of rupture of concrete is calculated using the well-known equation CODE NO. ECP 208-2005 [38].

$$f_{ctr} = 0.6\sqrt{f_{cu}} \qquad (3)$$

where f_{cu} is the compressive strength of concrete, N/mm².

3.2 Crack width in concrete

The crack width in a reinforced concrete slab is a significant limitation to measure the performance of structure. Fig. 17 illustrate the main crack width at the mid-span for (SS, SG, and SH (A, B and C)) tested slabs, respectively. The control slab SG had considerably more crack width at mid-span among all slabs tested due to the smaller axial stiffness of GFRP reinforcement than that of steel and HFRP reinforcement. For the GFRP slabs, wider cracks at the mid-span region are observed.

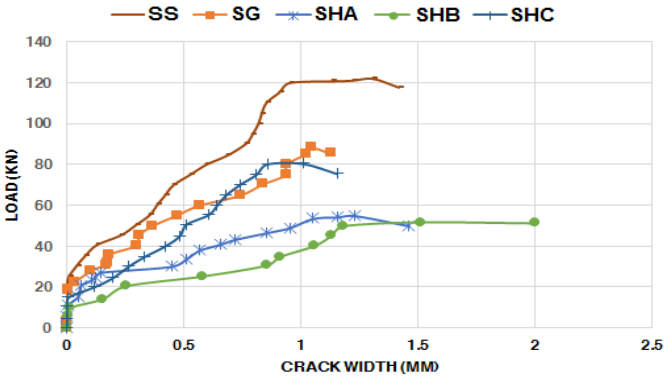

Fig. 17 Total applied load versus crack width of (SG, SS, and SH(A, B and C)) tested slabs

Table 3 TEST RESULTS AND FAILURE MODES

SLAB NOTATION	$E_r A_r d^2$ (10^8 KN/mm^{-2})	First cracking Load, P_{cr} (KN)		Failure load P_U (KN)	Under ultimate load, P_u (KN)		OBSERVED FAILURE MODE
		Exp.	Theo.		Crack width (mm)	Deflection(mm)	
S-S	19.097	32.5	32.49	122	1.22	36.9	Flexural-Tension Failure
G-S	3.914	27	29.49	88.5	1.98	35.4	Combined shear and flexure
SHA	4.058	28	30.43	57	1.463	38.4	Flexural-Tension Failure
SHB	4.443	31	34.11	52	1.512	30.1	Flexural-Tension Failure
SHC	4.87	28	31.29	80	1.156	36.3	Combined shear and flexure

* Defined As Lc/250, Where Ln Is The Length Of Clear Span Between The Supports Of The Slab, In Accordance With ECP 208-2005.

The hybrid slab SHC has lower crack width at mid-span among all hybrid tested slabs due to the increasing of axial stiffness that make it closer to SS specimen.

3.3 Load capacity

Failure loads of the tested slabs are presented in Fig.18. The failure load of the control slab S-G, which reinforced with normal GFRP bar is increased by 55.26%,70.1% and 10.625% of the total failure load of slabs SH (A, B and C), respectively. On the other hand, the failure load of the control slab SG was decreased by 27.45% of the failure load of slab SS. In spite of the same reinforcement ratio for all slabs; this slab resisted a failure load similar to that of slab SHC, and exhibited a higher load capacity than that of the other hybrid slabs except the control slabs S-S and SG which tolerated more loads than other slabs. Even though the innovative investigations of the reinforcement with the developed hybrid FRP bar achieve the target load capacity and achieve the ductility which is missing in the concrete member reinforced with FRP bar as general.

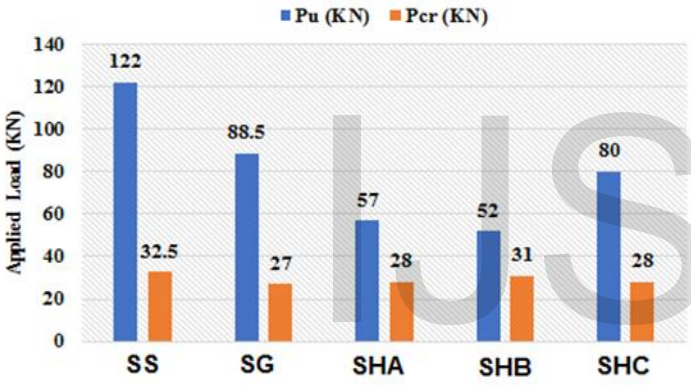

Fig. 18 Experimental crack load and load capacities of tested slabs

3.4 Load-Deflection Response

Fig. 20 to Fig. 24 illustrates the relationship between the applied load versus the recorded mid-span deflections. As expected theoretically, at early stages of loading, all slabs shown linear load-deflection behaviour before cracking due to the linear elastic characteristics of concrete and the reinforced bars. After cracking, there is a clear reduction in the flexural stiffness; as the load increased, the stiffness of slabs is reduced due to the occurrence of more additional cracks.

Also, as expected theoretically, the difference in mid-span deflections between the slabs can mainly be attributed to the differences in the flexural stiffness ($E_c I_e$, where E_c is the modulus of elasticity of concrete, N/mm^2, and I_e is the effective moment of inertia of the slab section, mm^4). For a cracked section, the flexural stiffness is proportional to $E_r A_r d^2$ in accordance with Matthys S., et.al, where E_r and A_r modulus of elasticity and cross-sectional area of the reinforcement, respectively, and d is the effective depth. An increase in the axial rigidity of the reinforcement may increases the value of $E_r A_r d^2$ and hence the flexural stiffness of the cracked section.

Table 3 show the magnitude of $E_r A_r d^2$ of the five slabs. It shows that slab SHC reinforced with HFRP-C has higher value in $E_r A_r d^2$ compared with the other slabs except S-S slab reinforced with steel which recording the highest value for $E_r A_r d^2$, this is due to the increase of modulus of elasticity of steel compared with the other used bars. At the deflection limit level ($L_c/250 \approx 8\ mm$), the applied load of slab SHC is around 80 KN, compared to 122 KN for conventional steel reinforced slab SS.

The mid-span deflections of the slabs can be predicted in accordance with ECP 208-2005 [38] and ACI 440.1R-15 [33].

Where L is the support span of the slab, mm, and P is the applied load, kN A modified expression for the effective moment of inertia is given by ACI 440.1R-15 [33] as follows, taking into account the effect of the modulus of elasticity of FRP tension reinforcement.

Due to the higher ductility of steel bars, SS slab demonstrated the biggest deflection of all tested slabs before yielding of steel. Overall, the type of hybrid FRP reinforcement slabs had a significant effect on the flexural stiffness and, consequently, deflections of the tested slabs. It could be noticed that slab SHA demonstrated higher deflection than SS slab as the mid-span flexural stiffness of slabs SS is higher than that of SH (A, B and C). The all under reinforced simply supported slabs showed acceptable large deflection compared with its span (>L/250). Fig. 25 present the deflection profile of tested slabs, deflection profile is measured along the length of tested slabs (at the center of slabs, 500 mm from the center along X-axis in both sides), the test results demonstrate the largest deflection of all tested slabs reinforced with hybrid bar (A, B and C) which hybridized by glass fiber and steel wires and they have a approached behavior to conventional reinforced slab with steel bar, that indicate the hybrid bars (A, B and C) have an approached performance of steel bar the ductility but there are significant shortage in the axial stiffness of the hybrid bars and (whereas the lowest deflection exhibited by the steel reinforced concrete slab).

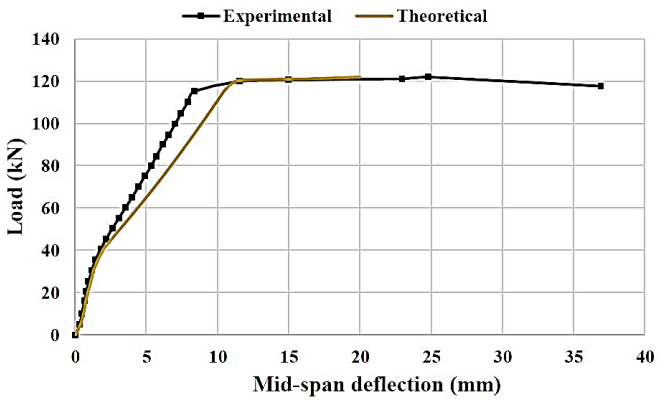

Fig. 19 Load-deflection at mid-span for SS slabs tested

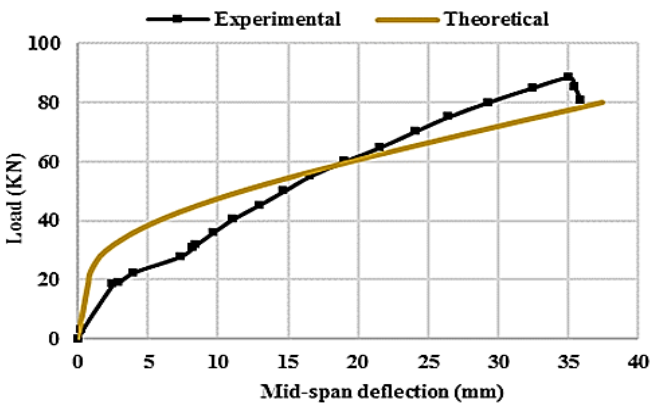

Fig. 20 Load-deflection at mid-span for SG slab

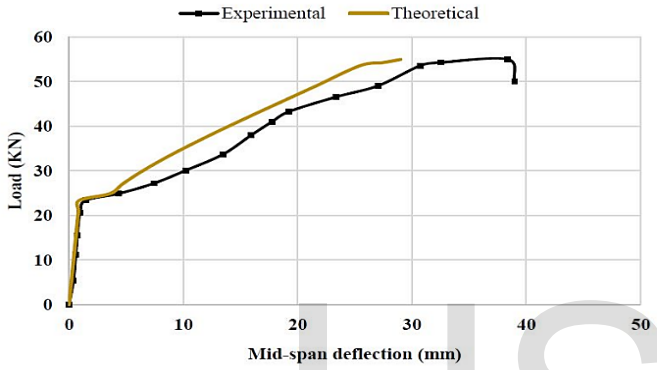

Fig. 21 Load-deflection at mid-span for SHA slab

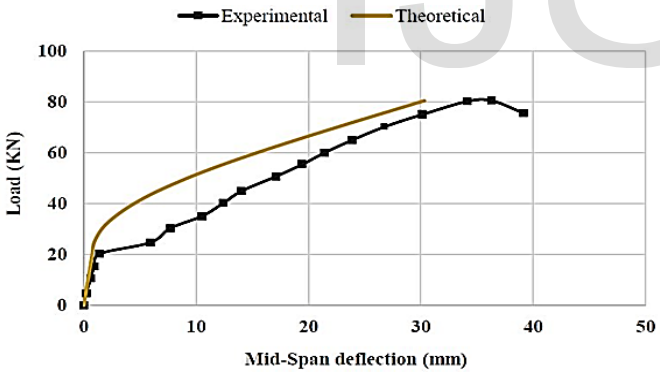

Fig. 22 Load-deflection at mid-span for SHC slab

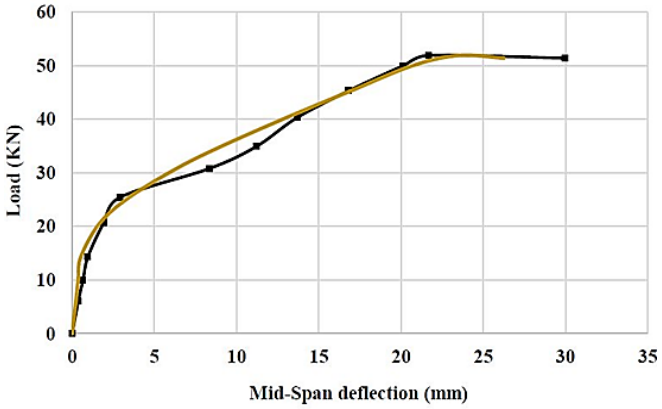

Fig. 23 Load-deflection at mid-span for SHB slab

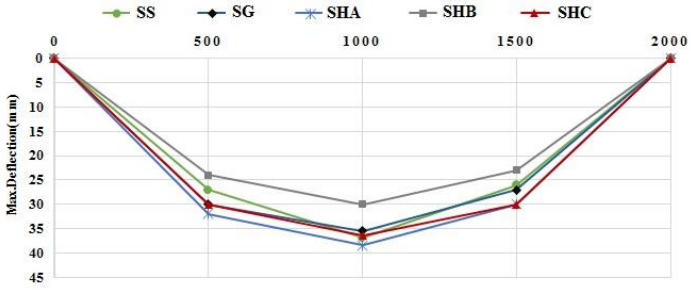

Fig. 24 Experimental deflection profile for all tested slabs

4 NON-LINEAR FINITE ELEMENTS ANALYSIS

Three dimensional non-linear finite element analysis is conducted to simulate the flexural behavior of the experimental program of concrete slabs reinforced with new developed HFRP bars. The commercially available finite element analysis software package, ANSYS (ANSYS release 13.0), is used in this process. The load-deflection curve is considered the key aspect in studying the hybrid slabs behavior as it involves response parameters including slab ultimate loads, first cracking load, and maximum deflection. Therefore, correlating the load-deflection relationships of the analytical results with that of the experimental ones is considered an effective mean to verify the non-linear model.

The load and boundary conditions for conventional and hybrid slabs are same and it is shown in the Fig. 26.

4.1 Modeling of Concrete and Reinforcement

A linear isotropic material model is used to represent the concrete. This material is known as quasi brittle material and has different behaviour in compression and tension. In this study, Solid 65 element is used to model the concrete. This element has eight nodes having three degrees of freedom at each node, i.e. translations in the nodal X, Y and Z directions respectively and the element is capable of cracking and crushing in three orthogonal directions.

A multilinear isotropic material model is used to represent steel reinforcements and a multilinear orthotropic material model was used to represent hybrid reinforcements. A link 180 element is used to model the reinforcement. It is two node elements and each node has three degrees of freedom. Translations are in the nodal X, Y and Z directions. This element is also capable of undergoing plastic deformation. The stress strain curve for reinforcement is obtained from bars tested in tension. The properties of hybrid bars are obtained from the experimental results.

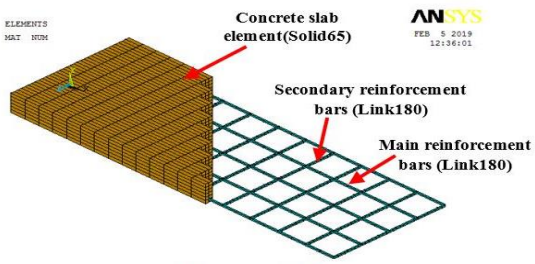

Fig. 25 Typical idealization of test Slab.

Table 4 Material properties of the proposed model.

(1) Concrete	
Concrete strength (f_c)	40,33,32,30 and 38 MPa ,respectively.
Young modulus of elasticity (E_c)	24149 to 26587 GPa
Poison's ratio (γ)	0.2
(2) Steel	
Maximum tensile strength (f_t)	600 MPa
Young modulus of elasticity (E_t)	2e5
Poison's ratio (γ)	0.3
(3) GFRP	
Maximum tensile strength (f_t)	575.22
Young modulus of elasticity (E_t)	--
Poison's ratio (γ)	0.2
(4) HFRP-A	
Maximum tensile strength (f_t)	300 MPa
Young modulus of elasticity (E_t)	42.5 GPa
Poison's ratio (γ)	0.25
(5) HFRP-B	
Maximum tensile strength (f_t)	331 MPa
Young modulus of elasticity (E_t)	46 GPa
Poison's ratio (γ)	0.25
(6) HFRP-C	
Maximum tensile strength (f_t)	575.22 MPa
Young modulus of elasticity (E_t)	54 GPa
Poison's ratio (γ)	0.25

4.2 Numerical model verification

A comparison is held among the numerical and experimental ultimate loads of the test specimens and listed in Table 4. As shown, good agreement between the experimental results and the proposed model is achieved. The results of non-linear FE analysis are compared to the experimental results of the tested slabs. For all the slabs, flexural cracks appeared when the concrete's tensile strength is exceeded and, consequently, the cracking moment is reached in the pure bending zone. Cracks are observed at the tension zone within and near the constant moment region.

The ratio of the analytical to experimental ultimate strength for the slabs ranged between 0.94 and 1.2, with a mean value of 1.088 and a C.O.V of 8.49%. Implicitly, the analysis reflected the significance of test parameters investigated on the load-carrying capacity. This variance is probably due in part to ignoring the effects of concrete toughening mechanisms and using assumed materials properties values instead of measured values.

Also, the average value of the ultimate deflection is found out as 0.878 mm for which the standard deviation is 0.167 mm and the coefficient of variation is 19.07 %.

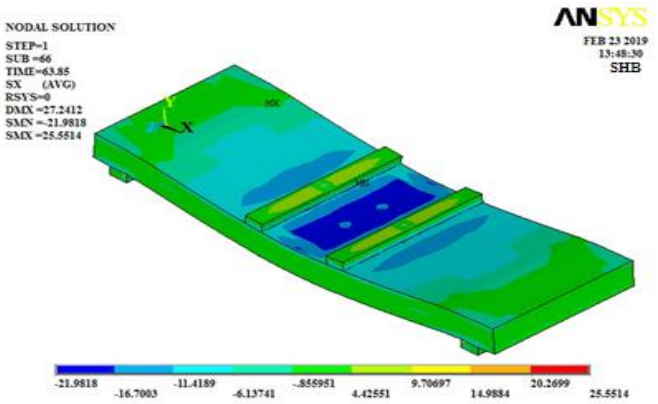

Fig. 26 Slab (SHB) stress profile of hybrid one way slabs reinforcement

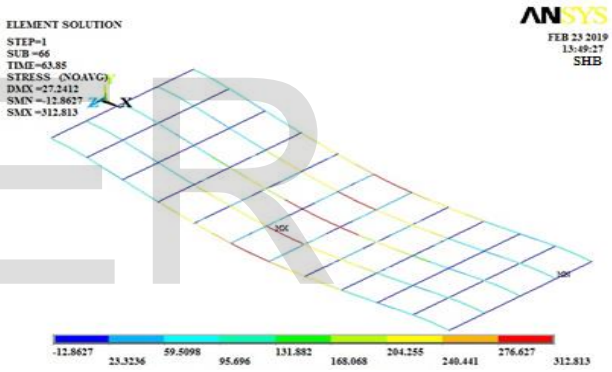

Fig. 27 Elastic stress profile of hybrid bar type-B

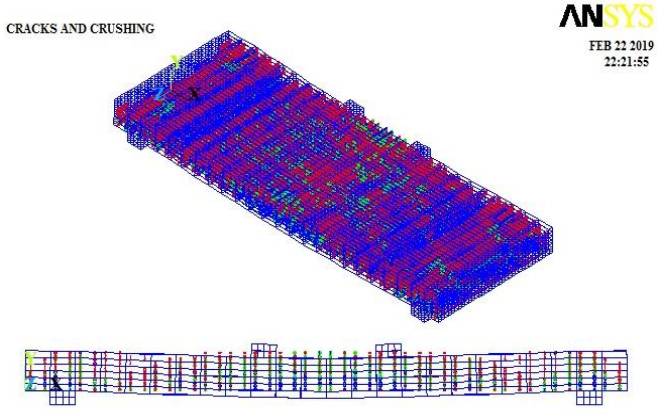

Fig. 28 Cracks propagation for Specimen (SHB)

Table 5 Comparison of test results with ANSYS results for all modelling slabs

Slab Notation	Failure load (kN)			Total Deformation (mm)			Failure mode
	Expt	FEA	P_{FEA} / P_{EXP}	Expt	FEA	$\Delta_{FEA}/\Delta_{EXP}$	
SS	120	121	1.08	36.9	29	0.786	F.F
SG	88.5	93.02	1.05	35.4	30	0.85	C.S.F
SHA	57	67	1.17	38.4	35	0.91	F.F
SHB	52	63	1.2	30.1	25	0.83	F.F
SHC	80	74.6	0.94	34	22	0.64	C.S.F
Mean			1.088			0.8032	
Standard deviation			0.09239			0.090824	
COV			0.084918			0.113077	

F.F: Flexural-Tension Failure at mid-span, and
C.S.F: Combined shear and flexure.

5 CONCLUSIONS

A semi-ductile hybrid HFRP composite rebars are developed as a unique product, which can be effectively used for infrastructure construction projects. The strength of the hybrid FRP rebar is lesser than that of conventional steel reinforcement but the semi-ductility is higher than any other types of FRP reinforcing products on the market. The hybrid FRP bars exhibited a bi-linear elastic behavior up to failure with a modulus of elasticity lesser than that of steel.

- The tensile test exposed that the hybridization of the GFRP and steel wires in core presented a large modulus of elasticity and low ultimate strength as compared to the GFRP bar. The bilinear behavior of the HFRP (Glass-steel wires) bar is specified semi-ductility as compared to the brittle failure of the normal GFRP bar at the ultimate state without any sign of fracture. Hybrid bars (Type A, B and C) specimen showed decrease up to 47.8% ,42.46% and 23.07%, respectively, as compared to that of the tensile strength of normal GFRP.
- The elastic modulus of the hybridized GFRP bar is increased by up to 24.4% with the material hybridization in comparison with the normal GFRP bar.
- The hybrid developed system is beneficial in terms of improving the serviceability and ductility of the concrete structure member but there is significant shortage in the axial stiffness of the hybrid bars. The load capacity of the hybrid slabs (SHA, SHB and SHC) decreased by as much as 35.6%,41.24% and 9.6%, respectively, as compared to the slab with normal GFRP bars.
- The slabs reinforced with hybrid FRP especially SHC slab undergoes similar deflection compared to the conventional slab. The yielding of hybrid reinforcement results in larger deformation at lower load rates leading to semi-ductile mode of failure but in the case of GFRP slab (SG) there is no yielding of reinforcements and hence the concrete fails by crushing prior to the reinforcements. It has been observed that the Hybrid reinforcement in tension side of the concrete slabs behave similar to the conventional reinforcements tested under pure tension.
- The hybrid slabs demonstrated an increase in curvature prior to collapse indicating the typical semi-ductile mode of failure where yielding of reinforcement followed by the crushing of concrete in compression. whilst in the case of GFRP slab (SG slab), there is no yielding of reinforcements.
- The hybrid slabs behavior exhibited adequate warning previous to failure through large and deep cracks, accompanied by large deformations. Also, the Crack widths and deflections of this slabs are significantly larger than the conventional slab, this is due to the low elastic modulus of HFRP bars in comparison to conventional steel reinforcement.
- The FE modeling approach based on material properties and failure modes obtained from experimental investigations could evaluate the bending performance of hybrid slabs. Results produced by the non-linear FE simulation and the theoretical value are nearly the same, and the non-linear FE result is slightly higher than the experimental value, which is caused by the deficiency of the specimens and other uncertain factors. A hybrid slab SHC is more appropriate form the different hybrid slabs types.

ACKNOWLEDGMENTS

The authors wish to acknowledge the financial support of the Civil Engineering Department, Faculty of Engineering Ain shams University, Cairo, Egypt. The first author is grateful of the chemical company sika Egypt, for supplied a free charge concrete admixture. Further investigation should be conducted to study the effect of the stress redistribution mechanism on the "semi-ductile" behavior regarding the quantity as well as the.

References

[1] H. Yalciner, O. Eren, and S. Sensoy, "An experimental study on the bond strength between reinforcement bars and concrete as a function of concrete cover, strength and corrosion level," Cement and Concrete Research, vol. 42, no. 5, pp. 643–655, 2012.

[2] F. Tondolo, "Bond behaviour with reinforcement corrosion, "Construction and Building Materials, vol. 93, pp. 926–932,2015.

[3] Jiang C, Wu YF, Dai MJ. Degradation of steel-to-concrete bond due to corrosion. Constr Build Mater 2018; 158:1073–80.

[4] L. Wang, C. Li, and J. Yi, "An experiment study on behavior of corrosion RC beams with different concrete strength," Journal of Coastal Research, vol. 73, pp. 259–264, 2015.

[5] Choi, O. C., Park, Y. S., & Ryu, H. Y. (2008). Corrosion evaluation of epoxy-coated bars by electrochemical impedance spectroscopy. International Journal of Concrete Structures and Materials, 2(2), 99–105.

[6] Guneyisi E, Gesoğlu M, Karaboğa F, Mermerdaş K. Corrosion behavior of reinforcing steel embedded in chloride contaminated concretes with and without metakaolin. Compo Part B 2013;45(1):1288–95.

[7] Berrocal CG, Fernandez I, Lundgren K, Lofgren I. Corrosion-induced cracking and bond behaviour of corroded reinforcement bars in SFRC. Compo Part B Eng. 2017; 113:123-37.

[8] Mariusz K. The experimental and innovative research on usability of Sulphur polymer composite for corrosion protection of reinforcing steel and concrete. Compo Part B Eng. 2011;42(5):1084–96.

[9] Blustein G, Rodriguez J, Romanogli R, Zinola CF. Inhibition of steel corrosion by calcium benzoate adsorption in nitrate solutions. Corros SCI 2005;47(2):369–83.

[10] Pebere N, Picaud T, Duprat M, Dabosi F, Pebere N, Picaud T. Evaluation of corrosion performance of coated steel by the impedance technique. Corrosion SCI 1989;29(9):1073–86.

[11] Manning David G. Corrosion performance of epoxy-coated reinforcing steel: north American experience. Constr. Build Mater 1996;10(5):349–65.

[12] Corrosion of metals in concrete. ACI222R-85. ACI J 1985. [January–February)].

[13] Kara IF, Ashour AF, Dundar C. Deflection of concrete structures reinforced with FRP bars. Compos Part B Eng 2013;44(1):375–84.

[14] Fan X, Zhang M. Behaviour of inorganic polymer concrete columns reinforced with basalt FRP bars under eccentric compression: an experimental study. Compos Part B Eng. 2016; 104:44–56.

[15] Wan B, Jiang C, Wu YF. Effect of defects in externally bonded FRP reinforced concrete. Constr Build Mater 2018; 172:63–76.

[16] Yu QQ, Wu YF. Fatigue retrofitting of cracked steel beams with CFRP laminates. Compo Struct 2018; 192:232–44.

[17] Li P, Wu YF, Zhou Y, Xing F. Cyclic stress-strain model for FRP-confined concrete considering post-peak softening. Compo Struct 2018; 201:902–15.

[18] El-Gamal, S. E., El-Salakawy, E. F., & Benmokrane, B. (2007). Influence of reinforcement on the behavior of concrete bridge deck slabs reinforced with FRP bars. ASCE, Journal of Composites for Construction, 11(5), 449–458.

[19] Nanni, A., Henneke, M. J., & Okamoto, T. (1994). Tensile properties of hybrid rods for concrete reinforcement. Construction and Building Materials, 8(1), 27–34.

[20] H. G. Harris, F. P. Hampton, S. Martin, and F. K. Ko, "Cyclic behavior of a second generation ductile hybrid fiber reinforced polymer (D-H-FRP) for earthquake resistant concrete structures," in Proceedings of 12th World Conference on Earthquake Engineering, p. 8, Auckland, New Zealand, January 2000.

[21] Hwang, J.-H., Seo, D.-W., Park, K.-T. and You, Y.-J. (2014) Experimental Study on the Mechanical Properties of FRP Bars by Hybridizing with Steel Wires. Engineering, 6, 365-373.

[22] D. W. Seo, K. T. Park, Y. J. You, and J. H. Hwang, "Evaluation for tensile performance of recently developed FRP hybrid bars," International Journal of Emerging Technology and Advanced Engineering, vol. 4, no. 6, pp. 631–637, 2014.

[23] D. W. Seo, K. T. Park, Y. J. You, and S. Y. Lee, "Experimental investigation for tensile performance of GFRP-steel hybridized rebar," Advances in Materials Science and Engineering, vol. 2016, Article ID 9401427, 12 pages, 2016.

[24] I. F. Kara, A. F. Ashour, and M. A. Koroglu, "Flexural behavior of hybrid FRP/steel reinforced concrete beams," Composite Structures, vol. 129, pp. 111–121, 2015.

[25] J. P. Won, C. G. Park, S. J. Lee, and B. T. Hong, "Durability of hybrid FRP reinforcing bars in concrete structures exposed to marine environments," International Journal of Structural Engineering, vol. 4, no. 1-2, pp. 63–74, 2013.

[26] Minkwan J., Sangyun L., and Cheolwoo P., (2017). Response of Glass Fiber Reinforced Polymer (GFRP)-Steel Hybrid Reinforcing Bar in Uniaxial Tension. International Journal of Concrete Structures and Materials, 2234-1315.

[27] J. P. Won and C. G. Park, "Effect of environmental exposure on the mechanical and bonding properties of hybrid FRP reinforcing bars for concrete structures," Journal of Composite Materials, vol. 40, no. 12, pp. 1063–1076, 2016.

[28] S. A. A. Mustafa and H. A. Hassan, "Behavior of concrete beams reinforced with hybrid steel and FRP composites," HBRC Journal, 2017, In press.

[29] Z. Sun, Y. Tang, Y. Luo, G. Wu, and X. He, "Mechanical properties of steel-FRP composite bars under tensile and compressive loading," International Journal of Polymer Science, vol. 2017, Article ID 5691278, 11 pages, 2017.

[30] Yingwu, Z., Yaowei, Z., Jun, P., Lili, S., Feng X., Hongfang, S., and Pengda, L. (2018). Experimental investigations on corrosion resistance of innovative steel-FRP composite bars using X-ray microcomputed tomography. Composites Part B 161 (2019) 272–284.

[31] National Housing & Building Research Center (NHBRC), http://www.hbrc.edu.eg

[32] ACI Committee 440. (2012). Guide test methods for fiber-reinforced polymers (FRPs) for reinforcing or strengthening concrete structures (ACI 440.3R-12).

[33] ACI Committee 440. (2015). Guide for the design and construction of concrete reinforced with FRP bars (ACI 440.1R-15).

[34] Farmington Hills, MI, USA: American Concrete Institute.

[35] ASTM D 3916. (2002). Standard test method for tensile properties of pultruded glass fiber reinforced plastic rods. West Conshohocken, PA: American Standard Test Method.

[36] CAN/CSA S806-12. (2012). Design and construction of building structures with fiber reinforced polymers. Ontario, Canada: Canadian Standards Association/National Standard of Canada.

[37] Egyptian Code of Practice for Reinforced Concrete Construction, ECP.203- 2007.

[38] Egyptian Code of practice for The use of fiber reinforced polymer (FRP) In the construction fields Code no. ECP 208-2005.